NUCLEAR MEDICINE

Iran J Radiol. 2019 April; 16(2):e68697. doi: 10.5812/iranjradiol.68697.

Published online 2019 January 23. **Research Article**

Ocular Biodistribution of ^{89}Zr-Bevacizumab in New Zealand Rabbits Determined Using PET/MRI: A Feasibility Study

Xiaoyuan Liu[1], Jianqiang Ye[2], Yan Zhang[3], Quan Liu[4], Ruizhen Bai[1], Wenbo Yuan[1], Dongyan Cai[4], Xiaoyuan Zheng[1], Yun Bian[1], Shijun Zhou[1], Juan Lv[1], Yongjuan Ding[1], Fen Xie[1], Hongwen Lu[1] and Bingxue Xie[1,3,*]

[1]Department of Pharmacy, Affiliated Hospital of Jiangnan University, Wuxi, China
[2]Department of Pathology, Wuxi Huishan District People's Hospital, Wuxi, China
[3]Department of Pharmacy, The Affiliated Wuxi Maternity and Child Health Care Hospital of Nanjing Medical University, Wuxi, Jiangsu, China
[4]Department of Oncology, Affiliated Hospital of Jiangnan University, Wuxi, China

[*]*Corresponding author*: Department of Pharmacy, Affiliated Hospital of Jiangnan University, Wuxi, China. Email: xiebingxue_ok@126.com

Received 2018 March 16; **Revised** 2018 December 12; **Accepted** 2018 December 18.

Abstract

Background: Despite studies on positron emission tomography/magnetic resonance imaging (PET/MRI) in oncological imaging with high soft-tissue contrast resolution, PET/MRI has not been studied in ophthalmology. ^{89}Zr-bevacizumab, designed as a probe for PET, targets vascular endothelial growth factor, which is highly expressed in ocular angiogenesis. Intravitreal injections of bevacizumab agents have curative effects on ocular disease.

Objectives: To study the ocular biodistribution of ^{89}Zr-bevacizumab in New Zealand rabbits using PET/MRI.

Materials and Methods: ^{89}Zr-bevacizumab, synthesized from conjugated bevacizumab and ^{89}Zr-oxalate, and the purity of radiolabeled antibodies were determined using radio high-performance liquid chromatography (radio-HPLC). Instant thin-layer chromatography (ITLC) was utilized to differentiate the labeled product from aggregates and unlabeled ^{89}Zr. ^{89}Zr-bevacizumab was injected 2 mm from the left limbus into the vitreous humor of six normal New Zealand white rabbits. Micro-PET was utilized for dynamic imaging from 5 minutes to 60 minutes postinjection and for static imaging at 4 hours, 24 hours, 48 hours, 120 hours, and 144 hours (10-minutes scans) postinjection. PET/MRI scans were fused using PMOD software.

Results: ^{89}Zr-bevacizumab with a radiochemical purity of 93.21% was monitored via PET imaging. Radioactivity levels in the eyes plateaued approximately 5 minutes after administration of ^{89}Zr-bevacizumab, and the measured vitreous values decreased from 340.52 $\pm$ 41.6% injected dose (ID)/g to 21.53 $\pm$ 3.39%ID/g by 144 hours. The half-life of the drug in the eye was calculated for 84.25 hours.

Conclusion: ^{89}Zr-bevacizumab could be monitored in animals by PET imaging, and the radiolabel exhibited high sensitivity in the vitreous body. Radioactivity levels in the eyes plateaued approximately 5 minutes after administration. This study clearly demonstrates the biodistribution of ^{89}Zr-bevacizumab.

Keywords: ^{89}Zr-Bevacizumab, PET-MRI, Eye, Distribution

1. Background

Positron emission tomography/magnetic resonance imaging (PET/MRI) has been studied in oncological imaging. The advantages of this approach include its lower ionizing radiation (1); high soft-tissue contrast resolution [e.g., for head and neck (2, 3), pelvic, and cervical cancer (4)]; and, in certain situations (e.g., cancer recurrence), a wider range of acquisition sequences compared with that of computed tomography (CT) (5). However, PET/MRI has not been studied in the context of ophthalmic examinations.

Vascular endothelial growth factor (VEGF), an effective endothelial cell mitogen, leads to the angiogenic growth of new blood vessels by stimulating proliferation, migration and tube formation (6). VEGF is vital in ocular angiogenesis and is highly expressed in retinopathy of prematurity (6), diabetic retinal disease (7) and aging diseases of the eye (8). In recent years, anti-VEGF treatment has become a first-line therapy in choroidal neovascularization (exudative maculopathy). This approach is also used (off-label) to treat corneal neovascularization (9, 10).

Bevacizumab, a humanized monoclonal full-length antibody involved in the antiangiogenic response, is targeted

to VEGF, and ^{89}Zr-bevacizumab is a probe designed for PET. Molecular imaging can be applied to visualize and potentially quantify functional differences between tumor and normal cells for primary breast cancer (11, 12), renal cell carcinoma (13), neuroendocrine tumors (14), ovarian cancer, and others (15, 16). Additionally, VEGF can be noninvasively visualized via PET imaging when the tracer ^{89}Zr-labeled bevacizumab is used.

Since VEGF is a crucial mediator of abnormal vascular permeability in retinopathy of prematurity, diabetic macular edema (17, 18) and age-related macular degeneration (ADM) (19, 20), the curative effects of intravitreal injections of bevacizumab agents are unsurprising. Although bevacizumab is not approved for ophthalmologic treatment, it is used in the treatment of exudative AMD despite being off-label for this application (21, 22). Bevacizumab demonstrated good efficacy and safety in a series of randomized clinical trials, producing results superior to those of laser photocoagulation of the macula with less myopia (23-25). For retinopathy of prematurity, bevacizumab treatment also has a positive effect, tending to improve vision; in this context, the morphological characteristics of retinal anatomy may predict visual function (26, 27). Despite the effects of bevacizumab in ocular treatment, the absorption and distribution of bevacizumab in eyes have rarely been studied. Traditionally, the distribution and duration of bevacizumab in rabbit eye tissues have been observed by immunofluorescence staining, which is invasive and can greatly differ across groups (28). PET/MRI allows for the noninvasive, quantitative, and repeatable acquisition of analytic information on molecules, biological processes and anatomical properties in living organisms (29).

2. Objectives

In this study, we aimed to assess the feasibility of PET/MRI to evaluate normal New Zealand white rabbit eyes with ^{89}Zr-bevacizumab as a probe. Furthermore, we aimed to study the ocular distribution of bevacizumab. PET/MRI represents a novel method for ophthalmic examination. Moreover, this study provides pharmacokinetic proof of the feasibility of utilizing bevacizumab in ocular treatment.

3. Materials and Methods

3.1. Conjugation and ^{89}Zr Labeling of Bevacizumab

^{89}Zr has a decay half-life of 78.4 hours, the mean β-energy is 395.5 keV, the positron branching fraction is 22.74%, and the main γ-emissions are 511 keV (45.5%) and 909 keV (99.04%). ^{89}Zr-bevacizumab was produced as previously described by Nagengast et al. (30). Briefly, bevacizumab was purified from excipients using a protein desalting 10 (PD10) column. Next, the conjugation of purified bevacizumab was achieved using deferoxamine (DFO). The ester and bevacizumab were conjugated at room temperature for 1 hour at pH 9 with 1.5 - 2.5 chelating groups per antibody molecule. Then, the mixture was purified again using a PD10 column. ^{89}Zr-oxalate was dissolved in oxalic acid, mixed for 3 minutes at pH 3.9 - 4.2, adjusted to pH 7 with sodium carbonate (Na_2CO_3), and then used for labeling. Modified bevacizumab was added and incubated in ^{89}Zr-oxalate solution for 40 minutes at room temperature. The crude product was purified with a PD10 column.

3.2. Quality Control for 89Zr-Bevacizumab

Modified bevacizumab was examined using high-performance liquid chromatography (HPLC). The HPLC parameters were a chromatographic column of 7.8 mm $\times$ 300 mm (TSK gel G3000SWXL), an ultraviolet (UV) wavelength of 280 nm, isocratic elution, a flow rate of 0.8 mL/min, and a mobile phase of 0.1 M phosphate-buffered saline (PBS) aqueous solution (pH 7.4). The radiochemical purity of radiolabeled antibodies was determined using radio-HPLC. Instant thin-layer chromatography (ITLC) (FLOW COUNT; Eckert & Ziegler), using 0.15 mol/L citrate buffer (pH 6.0) as the mobile phase, was utilized to differentiate the labeled product from aggregates and unlabeled ^{89}Zr.

3.3. Stability of ^{89}Zr-Bevacizumab

The stability of ^{89}Zr-bevacizumab was determined by storing the final product (1 mg, 50 megabecquerel [MBq]) at 4°C for 7 days. Radio-HPLC was performed 1 hour, 4 hours, 24 hours, 48 hours, 96 hours, and 168 hour after labeling.

3.4. MRI and Micro-PET

The work was conducted with the formal approval of the Beijing Association on Laboratory Animal Care. We anesthetized six rabbits with isoflurane (5% for induction and 1.5% - 2% for maintenance in 70% N_2O/30% O_2). The body temperature of each rabbit was maintained at 39°C. MR acquisition was initiated as soon as the rabbits were placed in supine position in the scanner. T2-weighted images (T2WI) were obtained prior to the injection of ^{89}Zr-bevacizumab into New Zealand white rabbits. PET images were acquired using a dedicated micro-PET system (BioCaliburn 700). After undergoing a 10-minutes transmission

scan, rabbits were injected 2 mm from the corneal limbus into the vitreous humor of the left eye with 25 μL 100 μCi ^{89}Zr-bevacizumab. PET was used for dynamic imaging from 5 minutes to 60 minutes and for static imaging at 4 hours, 24 hours, 48 hours, 120 hours, and 144 hours (10 minutes scans) after ^{89}Zr-bevacizumab injection.

An iterative ordered subset expectation maximization two-dimensional (OSEM-2D) algorithm was used to reconstruct the images. Attenuation and scatter corrections were applied. These parameters allowed for acquisition of the percent injected dose per gram of tissue-time (%ID-time) and standardized uptake value (SUV)-time curves for the eyes. PET image visualization, processing, and analyses were performed using PMOD software, version 3.1 (PMOD Technologies, Zurich, Switzerland).

3.5. Statistical Analyses

All quantitative data are expressed as the mean ± standard deviation (SD). An iterative OSEM-2D algorithm was used for reconstruction of the images. PET/MRI scans were fused using PMOD software, version 3.1.

4. Results

4.1. Radiolabeling and Quality Control

After bevacizumab was modified with DFO, the DFO-bevacizumab product had a chemical purity of 94.30%, as determined using HPLC (Figure 1). When marker production was complete, the radiochemical purity of the final product, ^{89}Zr-bevacizumab, was 93.21% as determined using radio-HPLC. The total proportion of polymer impurity was 6.79%, and free zirconium was not found (Figure 2). The specific activity of ^{89}Zr-bevacizumab was 58 MBq/mg. These results demonstrate that bevacizumab can be labeled with ^{89}Zr with high labeling efficiency.

The retention time and purity for bevacizumab were 9.900 minutes and 94.30%, respectively.

The retention time and radiochemical purity for ^{89}Zr-bevacizumab were 10.006 minutes and 93.21%, respectively.

4.2. In Vitro Evaluation of Radiolabeled Compounds

^{89}Zr-bevacizumab stored at 4°C exhibited a small decrease (4%) in protein-bound radioactivity after 168 hours.

4.3. PET/MRI Study of ^{89}Zr-Bevacizumab in Normal New Zealand White Rabbits

PET images acquired between 5 minutes and 144 hours after an injection of 25 μL 3.7 MBq ^{89}Zr-bevacizumab are shown below, including those obtained via dynamic imaging from 5 minutes to 60 minutes (Figure 3) and static imaging at 4 hours, 24 hours, 48 hours, 120 hours, and 144 hours (10 minutes scans) (Figure 4). Research was performed in accordance with National Institutes of Health (NIH) guidelines. Fused PET/MRI images revealed the temporal biodistribution of ^{89}Zr-bevacizumab in rabbit eyes.

In New Zealand white rabbits, a high level of radioactivity was observed in eyes (Figure 5A). The percent injected dose per gram of tissue (%ID/g)-time curves in Figure 5A show that the radioactivity level in eyes plateaued approximately 5 minutes after the administration of ^{89}Zr-bevacizumab. The SUV time curves in Figure 5B indicate the remaining quantities of ^{89}Zr-bevacizumab in rabbit eyes.

Radioactivity levels in eyes plateaued approximately 5 minutes after the ^{89}Zr-bevacizumab administration, and the measured vitreous values decreased from 340.52 ± 41.6% ID/g to 21.53 ± 3.39% ID/g by 144 hours. The drug half-life in eyes was calculated for 84.25 hours. Over time, ^{89}Zr-bevacizumab was detected from the injected area to the whole vitreous body. Moreover, a small amount may have entered the aqueous fluid, accompanied by a decrease in positron emission.

5. Discussion

Neovascularization occurs in several ocular diseases, such as exudative AMD (9), proliferative diabetic retinopathy (7), and retinopathy of prematurity (21). VEGF, a major factor inducing the formation of new vessels, acts via its receptors in ocular diseases. Anti-VEGF therapy is as an effective treatment for such diseases (9). For these diseases, early damage is often invisible upon clinical examination. VEGF-related approaches may allow for early examinations of ocular diseases.

^{89}Zr ($t_{1/2}$ = 78.4 hours), which has been exploited for PET studies of antibodies, has the advantages of facile labeling procedures and a relatively long decay time (16). Here, we utilized ^{89}Zr to evaluate the distribution of bevacizumab over 144 hours (1 week). We used PET/MRI instead of a traditional approach to study ocular pharmacokinetic properties. Using noninvasive PET/MRI technology, we observed the ocular biodistribution of bevacizumab in the vitreous chamber compartment of the same animal for as long as

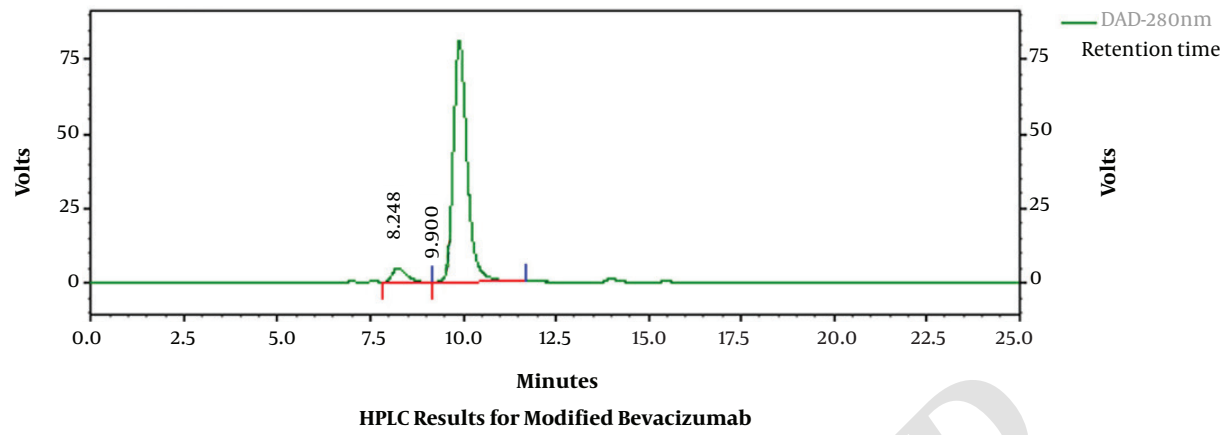

Figure 1. High-performance liquid chromatography (HPLC) results for modified bevacizumab

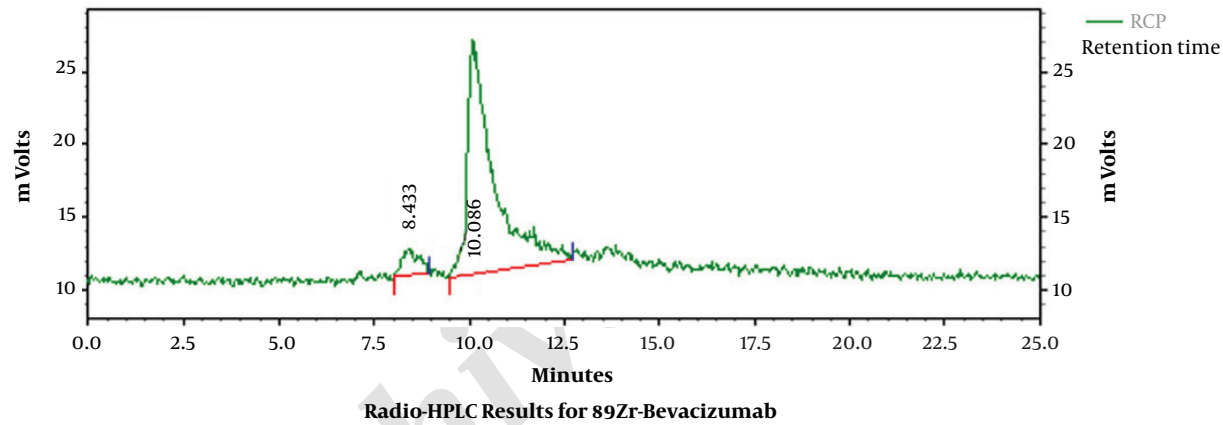

Figure 2. Radio- high-performance liquid chromatography (HPLC) results for ^{89}Zr-bevacizumab

144 hours following intravitreal administration. Isotope labeling is a new method for ocular pharmacokinetic studies. Since the blood-eye barrier may block bevacizumab in the bloodstream from entering the eyes, using traditional methods to track drugs in eyes is difficult.

In conclusion, ^{89}Zr-bevacizumab can be monitored via PET imaging in animals, and this radiolabeling approach exhibits high sensitivity in vitreous humors. Using noninvasive PET/MRI technology, we observed the ocular biodistribution of bevacizumab in the vitreous chamber compartment in the same animal for as long as 144 hours following intravitreal administration. This study clearly demonstrated the biodistribution of ^{89}Zr-bevacizumab. Moreover, PET/MRI represents a novel ophthalmic examination method.

Footnotes

Authors' Contributions: Xiaoyuan Liu and Jianqiang Ye contributed equally to the paper.

Conflict of Interests: The authors declared that they have no conflicts of interest regarding this study.

Ethical Considerations: Ethics Committee approval was obtained from the Institutional Ethics Committee of Affiliated Hospital of Jiangnan University to the commencement of the study.

Financial Disclosure: None declared.

Funding/Support: This study was supported by Wuxi Municipal Health Commission (project No.: Q201629 and NO: jzyx04) and Wuxi Hospital Management Center (project No.: YGZXQ1302).

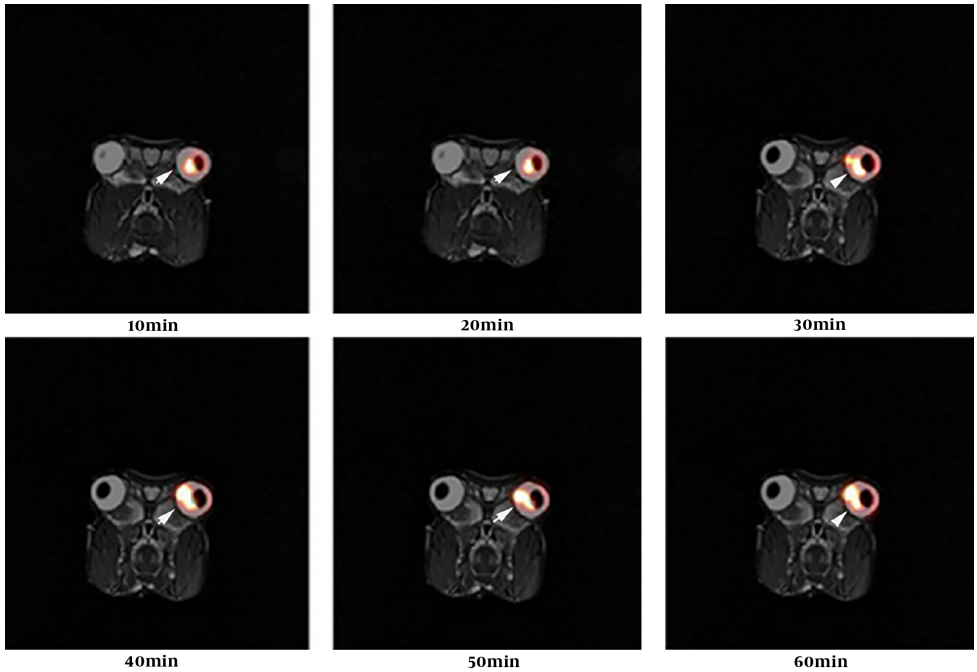

Figure 3. Fused positron emission tomography/magnetic resonance imaging (PET/MRI) images obtained via dynamic imaging from 5 minutes to 60 minutes after ^{89}Zr-bevacizumab injection

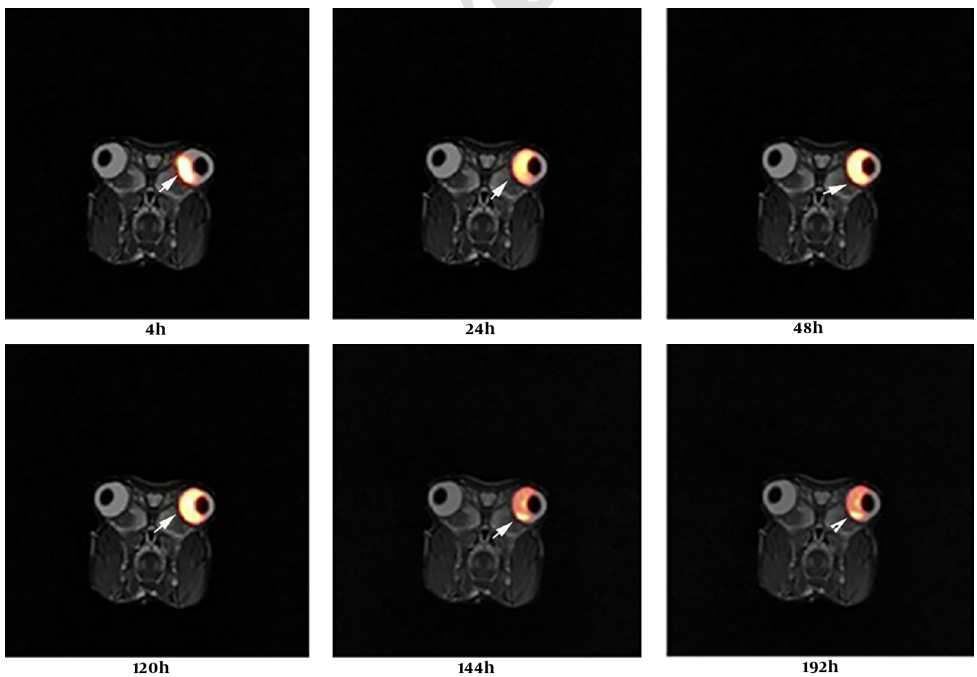

Figure 4. Fused positron emission tomography/magnetic resonance imaging (PET/MRI) images obtained via static imaging after ^{89}Zr-bevacizumab injection

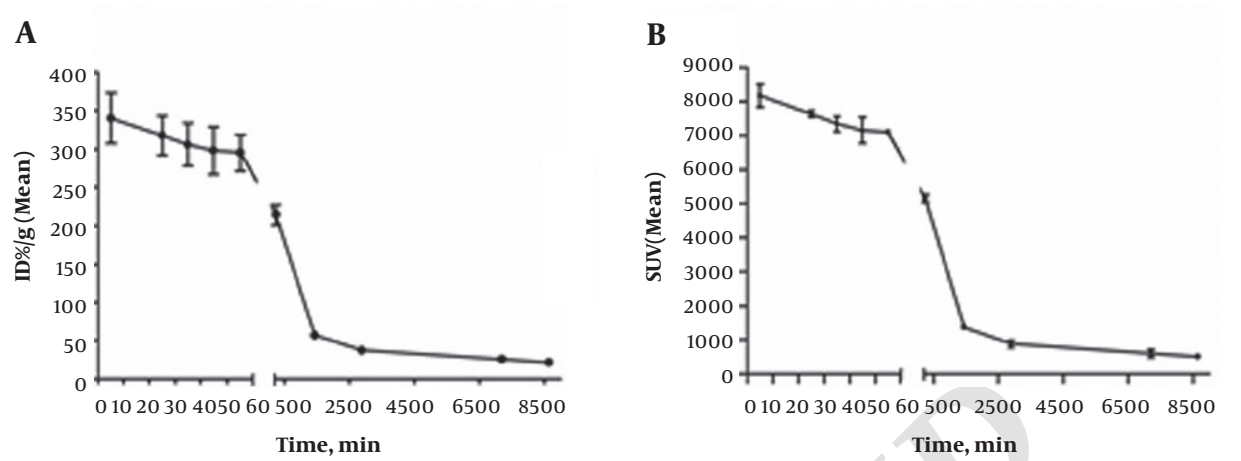

Figure 5. A, Percent injected dose per gram of tissue (%ID/g)-time (minutes) curves. B, Standardized uptake value (SUV) (mean)-time curves for positron emission tomography (PET) images acquired via dynamic imaging from 5 minutes to 60 minutes and static imaging at 4 hours, 24 hours, 48 hours, 120 hours, and 144 hours.

References

1. Bashir U, Mallia A, Stirling J, Joemon J, MacKewn J, Charles-Edwards G, et al. PET/MRI in oncological imaging: State of the art. *Diagnostics (Basel)*. 2015;**5**(3):333–57. doi: 10.3390/diagnostics5030333. [PubMed: 26854157]. [PubMed Central: PMC4665605].
2. Garibotto V, Heinzer S, Vulliemoz S, Guignard R, Wissmeyer M, Seeck M, et al. Clinical applications of hybrid PET/MRI in neuroimaging. *Clin Nucl Med*. 2013;**38**(1):e13–8. doi: 10.1097/RLU.0b013e3182638ea6. [PubMed: 23242058].
3. Lee SJ, Seo HJ, Cheon GJ, Kim JH, Kim EE, Kang KW, et al. Usefulness of integrated PET/MRI in head and neck cancer: a preliminary study. *Nucl Med Mol Imaging*. 2014;**48**(2):98–105. doi: 10.1007/s13139-013-0252-2. [PubMed: 24900149]. [PubMed Central: PMC4028474].
4. Khiewvan B, Torigian DA, Emamzadehfard S, Paydary K, Salavati A, Houshmand S, et al. Update of the role of PET/CT and PET/MRI in the management of patients with cervical cancer. *Hell J Nucl Med*. 2016;**19**(3):254–68. doi: 10.1967/s002449910409. [PubMed: 27824966].
5. Aras M, Ones T, Dane F, Nosheri O, Inanir S, Erdil TY, et al. False positive FDG PET/CT resulting from fibrous dysplasia of the bone in the work-up of a patient with bladder cancer: case report and review of the literature. *Iran J Radiol*. 2012;**10**(1):41–4. doi: 10.5812/iranjradiol.10303. [PubMed: 23599713]. [PubMed Central: PMC3618905].
6. Penn JS, Madan A, Caldwell RB, Bartoli M, Caldwell RW, Hartnett ME. Vascular endothelial growth factor in eye disease. *Prog Retin Eye Res*. 2008;**27**(4):331–71. doi: 10.1016/j.preteyeres.2008.05.001. [PubMed: 18653375]. [PubMed Central: PMC3682685].
7. Ajlan RS, Silva PS, Sun JK. Vascular endothelial growth factor and diabetic retinal disease. *Semin Ophthalmol*. 2016;**31**(1-2):40–8. doi: 10.3109/08820538.2015.1114833. [PubMed: 26959128].
8. Marneros AG. Increased VEGF-A promotes multiple distinct aging diseases of the eye through shared pathomechanisms. *EMBO Mol Med*. 2016;**8**(3):208–31. doi: 10.15252/emmm.201505613. [PubMed: 26912740]. [PubMed Central: PMC4772957].
9. Kovach JL, Schwartz SG, Flynn HW Jr, Scott IU. Anti-VEGF treatment strategies for wet AMD. *J Ophthalmol*. 2012;**2012**:786870. doi: 10.1155/2012/786870. [PubMed: 22523653]. [PubMed Central: PMC3317200].
10. Mirabelli P, Peebo BB, Xeroudaki M, Koulikovska M, Lagali N. Early effects of dexamethasone and anti-VEGF therapy in an inflammatory corneal neovascularization model. *Exp Eye Res*. 2014;**125**:118–27. doi: 10.1016/j.exer.2014.06.006. [PubMed: 24933712].
11. Gaykema SB, Brouwers AH, Lub-de Hooge MN, Pleijhuis RG, Timmer-Bosscha H, Pot L, et al. 89Zr-bevacizumab PET imaging in primary breast cancer. *J Nucl Med*. 2013;**54**(7):1014–8. doi: 10.2967/jnumed.112.117218. [PubMed: 23651946].
12. Gaykema SB, Schroder CP, Vitfell-Rasmussen J, Chua S, Oude Munnink TH, Brouwers AH, et al. 89Zr-trastuzumab and 89Zr-bevacizumab PET to evaluate the effect of the HSP90 inhibitor NVP-AUY922 in metastatic breast cancer patients. *Clin Cancer Res*. 2014;**20**(15):3945–54. doi: 10.1158/1078-0432.CCR-14-0491. [PubMed: 25085789].
13. Oosting SF, Brouwers AH, van Es SC, Nagengast WB, Oude Munnink TH, Lub-de Hooge MN, et al. 89Zr-bevacizumab PET visualizes heterogeneous tracer accumulation in tumor lesions of renal cell carcinoma patients and differential effects of antiangiogenic treatment. *J Nucl Med*. 2015;**56**(1):63–9. doi: 10.2967/jnumed.114.144840. [PubMed: 25476536].
14. van Asselt SJ, Oosting SF, Brouwers AH, Bongaerts AH, de Jong JR, Lub-de Hooge MN, et al. Everolimus reduces (89)Zr-bevacizumab tumor uptake in patients with neuroendocrine tumors. *J Nucl Med*. 2014;**55**(7):1087–92. doi: 10.2967/jnumed.113.129056. [PubMed: 24790218].
15. van der Bilt AR, Terwisscha van Scheltinga AG, Timmer-Bosscha H, Schroder CP, Pot L, Kosterink JG, et al. Measurement of tumor VEGF-A levels with 89Zr-bevacizumab PET as an early biomarker for the antiangiogenic effect of everolimus treatment in an ovarian cancer xenograft model. *Clin Cancer Res*. 2012;**18**(22):6306–14. doi: 10.1158/1078-0432.CCR-12-0406. [PubMed: 23014526].
16. Nagengast WB, de Korte MA, Oude Munnink TH, Timmer-Bosscha H, den Dunnen WF, Hollema H, et al. 89Zr-bevacizumab PET of early antiangiogenic tumor response to treatment with HSP90 inhibitor NVP-AUY922. *J Nucl Med*. 2010;**51**(5):761–7. doi: 10.2967/jnumed.109.071043. [PubMed: 20395337].
17. Aiello LP, Avery RL, Arrigg PG, Keyt BA, Jampel HD, Shah ST, et al. Vascular endothelial growth factor in ocular fluid of patients with diabetic retinopathy and other retinal disorders. *N Engl J Med*. 1994;**331**(22):1480–7. doi: 10.1056/NEJM199412013312203. [PubMed: 7526212].

18. Antonetti DA, Barber AJ, Hollinger LA, Wolpert EB, Gardner TW. Vascular endothelial growth factor induces rapid phosphorylation of tight junction proteins occludin and zonula occluden 1. A potential mechanism for vascular permeability in diabetic retinopathy and tumors. *J Biol Chem*. 1999;**274**(33):23463–7. doi: 10.1074/jbc.274.33.23463. [PubMed: 10438525].
19. Gamulescu MA, Radeck V, Lustinger B, Fink B, Helbig H. Bevacizumab versus ranibizumab in the treatment of exudative age-related macular degeneration. *Int Ophthalmol*. 2010;**30**(3):261–6. doi: 10.1007/s10792-009-9318-7. [PubMed: 19633973].
20. Schmucker C, Antes G, Lelgemann M. A systematic review on the effect of bevacizumab in exudative age-related macular degeneration. *Graefes Arch Clin Exp Ophthalmol*. 2010;**248**(3):451–2. author reply 453-4. doi: 10.1007/s00417-009-1249-5. [PubMed: 20012081].
21. Hwang CK, Hubbard GB, Hutchinson AK, Lambert SR. Outcomes after intravitreal bevacizumab versus laser photocoagulation for retinopathy of prematurity: A 5-year retrospective analysis. *Ophthalmology*. 2015;**122**(5):1008–15. doi: 10.1016/j.ophtha.2014.12.017. [PubMed: 25687024]. [PubMed Central: PMC4414677].
22. Scott IU, Edwards AR, Beck RW, Bressler NM, Chan CK; Diabetic Retinopathy Clinical Research Network, et al. A phase II randomized clinical trial of intravitreal bevacizumab for diabetic macular edema. *Ophthalmology*. 2007;**114**(10):1860–7. doi: 10.1016/j.ophtha.2007.05.062. [PubMed: 17698196]. [PubMed Central: PMC2245885].
23. Michaelides M, Kaines A, Hamilton RD, Fraser-Bell S, Rajendram R, Quhill F, et al. A prospective randomized trial of intravitreal bevacizumab or laser therapy in the management of diabetic macular edema (BOLT study) 12-month data: Report 2. *Ophthalmology*. 2010;**117**(6):1078–1086 e2. doi: 10.1016/j.ophtha.2010.03.045. [PubMed: 20416952].
24. Gillies MC, Lim LL, Campain A, Quin GJ, Salem W, Li J, et al. A randomized clinical trial of intravitreal bevacizumab versus intravitreal dexamethasone for diabetic macular edema: The BEVORDEX study. *Ophthalmology*. 2014;**121**(12):2473–81. doi: 10.1016/j.ophtha.2014.07.002. [PubMed: 25155371].
25. Dorta P, Kychenthal A. Spectral-domain optical coherence tomography of the macula in preterm infants treated with bevacizumab for retinopathy of prematurity. *Ophthalmic Surg Lasers Imaging Retina*. 2015;**46**(3):321–6. doi: 10.3928/23258160-20150323-04. [PubMed: 25856817].
26. Chen SN, Lian I, Hwang YC, Chen YH, Chang YC, Lee KH, et al. Intravitreal anti-vascular endothelial growth factor treatment for retinopathy of prematurity: Comparison between ranibizumab and bevacizumab. *Retina*. 2015;**35**(4):667–74. doi: 10.1097/IAE.0000000000000380. [PubMed: 25462435].
27. Kong L, Bhatt AR, Demny AB, Coats DK, Li A, Rahman EZ, et al. Pharmacokinetics of bevacizumab and its effects on serum VEGF and IGF-1 in infants with retinopathy of prematurity. *Invest Ophthalmol Vis Sci*. 2015;**56**(2):956–61. doi: 10.1167/iovs.14-15842. [PubMed: 25613938].
28. Ye Z, Ji YL, Ma X, Wen JG, Wei W, Huang SM. Pharmacokinetics and distributions of bevacizumab by intravitreal injection of bevacizumab-PLGA microspheres in rabbits. *Int J Ophthalmol*. 2015;**8**(4):653–8. doi: 10.3980/j.issn.2222-3959.2015.04.02. [PubMed: 26309857]. [PubMed Central: PMC4539635].
29. Jang BS. MicroSPECT and MicroPET imaging of small animals for drug development. *Toxicol Res*. 2013;**29**(1):1–6. doi: 10.5487/TR.2013.29.1.001. [PubMed: 24278622]. [PubMed Central: PMC3834443].
30. Nagengast WB, de Vries EG, Hospers GA, Mulder NH, de Jong JR, Hollema H, et al. In vivo VEGF imaging with radiolabeled bevacizumab in a human ovarian tumor xenograft. *J Nucl Med*. 2007;**48**(8):1313–9. doi: 10.2967/jnumed.107.041301. [PubMed: 17631557].